SUPPORTING INFORMATION

Combined Theoretical and Experimental Investigation of Lewis Acid-Carbonyl Interactions for Metathesis

Tanmay Malakar,[†] Carly S. Hanson,[‡] James J. Devery, III,*[‡] Paul M. Zimmerman*[†]

[†]Department of Chemistry, University of Michigan, 930 North University Avenue, Ann Arbor, MI 48109, USA.

[‡]Department of Chemistry & Biochemistry, Loyola University Chicago, Flanner Hall, 1068 West Sheridan Road, Chicago, Illinois 60660, USA

*paulzim@umich.edu, *jdevery@luc.edu

Contents:

S1. General Information

General Laboratory Procedures. All moisture-sensitive reactions were performed under an atmosphere of argon in flame-dried round bottom flasks or glass vials fitted with rubber septa. Stainless steel syringes were used to transfer air or moisture-sensitive liquids.

Materials and Instrumentation. All chemicals were purchased from Sigma-Aldrich, VWR, Beantown, or Acros and were used as received unless otherwise stated. Benzaldehyde was distilled and stored over 3 Å molecular sieves and DCE was stored over 3 Å molecular sieves. Solution infrared (IR) spectra were obtained using a Mettler Toledo ReactIR 15 and solid-state IR spectra were obtained using a Nexsus 470 FT-IR/ATR with a Smart Endurance attachment. IR data are represented as frequency of absorption (cm^{-1}).

Abbreviations used: DCE = 1,2-dichloroethane

S2. Computational Details

All quantum chemical calculations utilize density functional theory (DFT) as implemented in the Q-Chem 5.1 electronic structure program.[1] Geometry optimizations were carried out using the B97-D[2] density functional employing the double-ζ, 6-31+G* basis set. Initial transition state (TS) searches were performed using the reaction discovery tools of the Zimmerman group, in particular, the double-ended Growing String Method (GSM).[3-5] GSM locates minimum energy reaction paths and the associated transition states, without requiring detailed prior knowledge of the transition state structures. To ascertain the true nature of all stationary points, normal mode analysis was conducted at the B-97D/6-31+G* level of theory. These frequency computations were further used

to assign theoretical IR spectra of the predicted structures. Following this, single point solvent phase calculation on the gas phase optimized geometries were performed using the SMD[6] solvent model, with 1,2-dichloroethane (DCE) as the solvent. SMD energies were computed using the ωB97X-D3[7] density functional and the def2-TZVP basis set in the ORCA quantum chemical package.[8] Noncovalent interaction (NCI) analysis was performed using NCIPLOT program.[9]

Thermal corrections to enthalpies (H_{corr}) and Gibbs free energies (G_{corr}) were obtained from the respective frequency calculation in the gas phase. For the solvent phase free energies, entropic corrections are significantly quenched in the solvent phase as compared to those in the gas phase. Experiments have shown solutes lose about 50%-60% of their entropy on going from the gas phase to the solution phase. Therefore, the correction scheme based on works by Wertz and Ziegler and others was used, where the entropy of any solute is estimated to be 0.5 S(g), with S(g) being the entropy of the solute in the gas phase.[10-12] Furthermore, correction (1.90 kcal mol^{-1}, at 298 K)[13] due to standard state concentration (1M) were added to these G(l). Reported energies for intermediates and activation barriers are solvent phase (DCE) free energies obtained using the ωB97X-D3/def2-TZVP level of theory in the high spin sextet state unless mentioned otherwise.

The gas-phase entropy is given by,

$$-S(g) = \frac{G(g) - H(g)}{T} = \frac{G_{corr} - H_{corr}}{T}$$

$$S(l) = 0.5 * S(g)$$

$H(l) = E(l) + H_{corr}$, E(l) is solvent phase total energy.

Therefore,

$$G(l) = [H(l) + S(l)] + [1.9\ kcal\ mol^{-1}]$$

S3. Spectral features of Metal-Ac complexes

The solution-phase behavior for the **Fc-Ac** system is consistent with what is observed for $GaCl_3$, which displays no aggregation behavior in our hands. We observe similar behavior for BF_3, $InCl_3$, $ZrCl_4$, and $AlCl_3$.[14] In particular for $FeCl_3$, $GaCl_3$, and $AlCl_3$, the peak at 1633 cm^{-1} consistent with the Lewis pair reaches a maximum when 1 equiv of **Ac** is added to the solution. Further, $FeCl_3$ and $AlCl_3$ form homogeneous solutions when 1 equiv **Ac** is present. We also observe similar peak widths for acetophenone and ethyl acetate. This analysis is consistent with observations by Susz[15-17], by Greenwood[18-19], and by Kochi[21]. Lastly, peak broadening is common when intermolecular interactions that allow for exchange are present in the observed sample (i.e. hydrogen bonding), and we have previously demonstrated that the binding affinity of **Be** to **Fc** is much higher than **Ac**, based on observation of solution conductivity[14] as well as byproduct inhibition observations in carbonyl-olefin metathesis kinetic studies.[21]

S4. Gas phase vs Solvent phase optimized structures of Fc-carbonyl complexes

Gas-phase optimized structures of the ion-pairs (species **15**, **16** and **20**, **21**) might differ from the solvent phase. However, when the gas phase optimized geometries are overlaid with the corresponding solvent phase optimized structures, the geometries superimpose with each other, and low RMSD values also result (see below).

Species	Overlay structures	RMSD (Å)
15	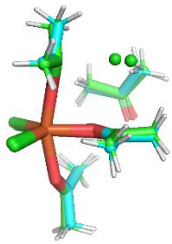	0.20
16	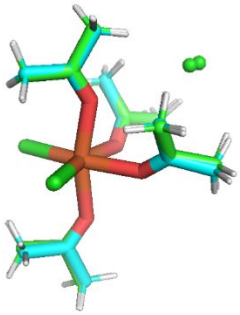	0.12
20	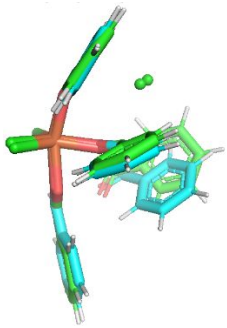	0.27
21	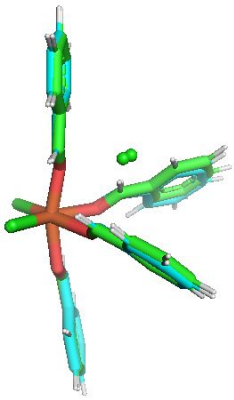	0.12

Comparison of gas-phase optimization to solvent-phase optimization for key structures.

S5. Wiberg bond order analysis

Wiberg bond order analysis[22] of complexes **12**, **13**, and **14** is given below for the bonds associated with the chloride migration.

Species	Fe-Cl bond	[b]C-Cl
12	1.41	0.0
13	0.07	0.90
14	0.05	0.80

[b]carbonyl carbon of acetone close to the chloride ion.

The reduction in bond order from 1.41 to 0.05 for the transformation of **12** into **14** suggests that the Fe-Cl bond is completely broken and simultaneously the C-Cl bond (weak) is started to form. This further ascertains that the chloride is migrating from the primary coordination sphere of the metal center.

S6. Spectral overlap between free Ac and complex 14, 15

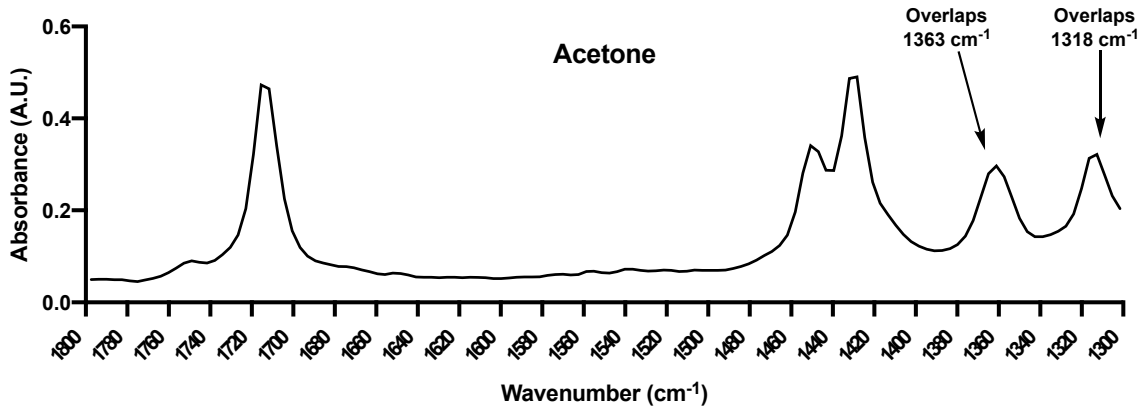

Our model predicts that **14** will have a vibration at 1318 cm^{-1} and **15** will have a vibration at 1363 cm^{-1}. Both peaks have significant overlap with free **Ac**. Hence, it is not possible to resolve whether these peaks are present.

S7. Experimental titration data for Fc-Ac complexes

Table S1. Experimental concentration (M) of the species detected in the titration of **Fc-Ac** complexes.

Equiv. Ac added	[11]	[free Ac]	[15+16]
1.4	1.24E-01	1.18E-02	3.96E-02
1.5	1.20E-01	2.76E-02	4.33E-02
1.6	1.18E-01	5.84E-02	4.56E-02
1.8	1.16E-01	6.01E-02	4.74E-02
1.9	1.14E-01	7.78E-02	4.86E-02
2.0	1.12E-01	8.48E-02	5.11E-02
2.3	9.91E-02	1.93E-01	6.28E-02
2.6	9.14E-02	3.03E-01	6.99E-02
3.0	8.55E-02	3.90E-01	7.51E-02
3.3	8.02E-02	4.88E-01	7.98E-02
3.6	7.81E-02	5.39E-01	8.13E-02
4.0	7.57E-02	6.07E-01	8.30E-02
4.3	7.26E-02	6.80E-01	8.55E-02
4.6	7.07E-02	7.37E-01	8.68E-02
5.0	6.91E-02	8.00E-01	8.77E-02
5.6	6.68E-02	8.74E-01	8.88E-02
6.3	6.58E-02	9.41E-01	8.87E-02
9.6	6.19E-02	1.18E+00	8.68E-02

S8. Experimental ΔG for the transformation of 1:1 complex 11 in to the 4:1 complex 15 and 16 in case of Ac.

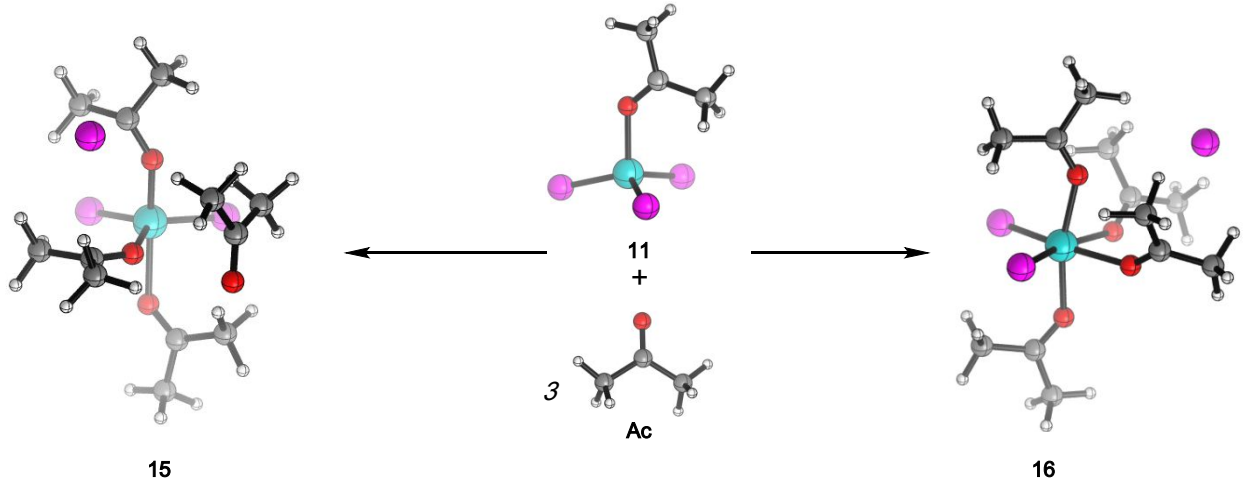

Here, we have the following expression for the Gibbs free energy change,

$$\Delta G = \Delta G^0 + RT(lnQ).....(S1) \quad Q = \frac{[15+16]}{[11]\,[Ac]^3}$$

Where, Q is reaction quotient, R universal gas constant, and T is temperature.

At equilibrium,

$$\Delta G = \Delta G^0 + RT(lnK_{Eq}).....(S2) \quad K_{Eq} = \frac{[15+16]_{Eq}}{[11]_{Eq}[Ac]_{Eq}^3}$$

$$\Delta G^0 = -RT(lnK_{Eq}).....(S3)\ ,\ \Delta G = 0, at\ equilibrium$$

Let us, assume that at 9.6 equiv (last entry, Table S1) **Ac** addition the system attained equilibrium. Then,

$$[15+16]_{Eq} = 8.68 * 10^{-2}\ M$$

$$[11]_{Eq} = 6.19 * 10^{-2}\ M$$

$$[Ac]_{Eq} = 1.18\ M$$

$$\Delta G^0 = 0.1\ kcal/mol\ .....\ (S4)\ ,\ T = 298.15\ K$$

From Table S1,

$$average\ Q = 1.22 * 10^4$$

Then from eq. 1, we have,

$$\Delta G = \Delta G^0 + RT * ln(1.22 * 10^4)$$

$$\Delta G = 5.6\ kcal/mol\ ,\ T = 298.15\ K$$

Note that our quantum chemical simulations predicted two possible 4:1 Lewis complexes of which **16** is 7.7 kcal/mol more stable than **15**. Hence, it can be anticipated that the reaction system will largely be populated by the species **16** at superstochiometric carbonyl addition. Thus, the theoretically predicted Gibbs free energy (ΔG = +9.8 kcal/mol, Figure 3b right, see in the main manuscript) for the formation of **16** deviates from the experimental results (ΔG = +5.6 kcal/mol) by only 4.2 kcal/mol.

S9. Thermodynamics for the formation of species 19

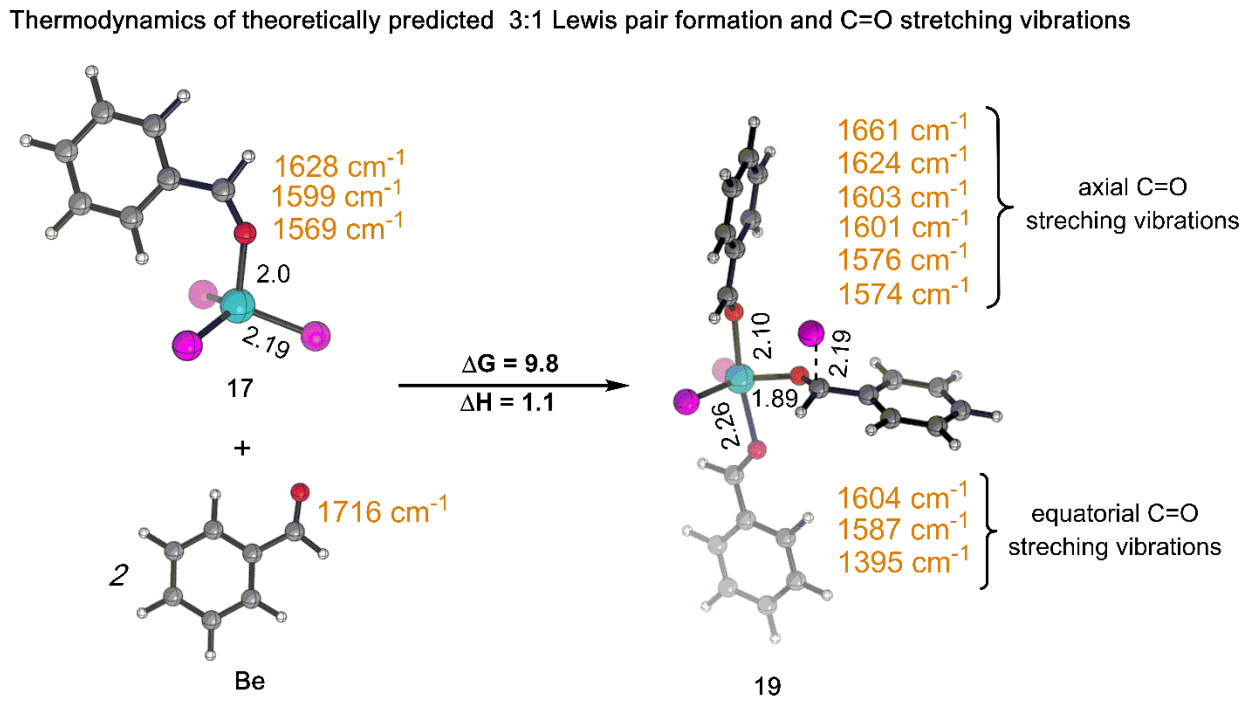

Figure S1: Theoretically predicted thermodynamics and C=O IR stretching frequency (cm^{-1}) of the 3:1 complex **19** formed from **Fc** and **Be**. Reaction energies (kcal/mol) were obtained at ωb97X-D3/def2-TZVP/SMD(DCE) level of theory. Color code: Fe cyan, Cl magenta, O red, C grey, H white respectively

S10. Experimental titration data for Fc-Be complexes

Table S2. Experimental concentration (M) of the species detected in the titration of **Fc-Be** complexes.

Equiv. Be added	[17]	[free Be]	[19+20]
1.08	1.30E-01	9.94E-03	3.37E-02
1.18	1.27E-01	1.45E-02	3.64E-02
1.27	1.22E-01	1.88E-02	4.07E-02
1.37	1.18E-01	2.56E-02	4.52E-02
1.47	1.12E-01	2.93E-02	5.07E-02
1.57	1.06E-01	3.49E-02	5.62E-02
1.67	1.01E-01	4.23E-02	6.09E-02
1.76	9.65E-02	5.13E-02	6.54E-02
1.86	9.19E-02	5.88E-02	6.97E-02
1.96	8.83E-02	6.69E-02	7.30E-02
2.45	7.44E-02	1.19E-01	8.56E-02
2.94	6.57E-02	1.89E-01	9.30E-02
3.43	6.31E-02	2.59E-01	9.44E-02
3.92	5.91E-02	3.06E-01	9.71E-02
4.41	5.91E-02	3.54E-01	9.59E-02
4.90	5.83E-02	3.99E-01	9.55E-02
5.39	6.56E-02	4.80E-01	8.70E-02
5.88	5.90E-02	5.09E-01	9.25E-02
6.37	6.18E-02	5.59E-01	8.86E-02
6.86	5.85E-02	5.91E-01	9.08E-02
9.31	5.62E-02	7.56E-01	8.77E-02

S11. Experimental ΔG for the transformation of 1:1 complex 17 in to the 4:1 complex 19 and 20 in the case Be.

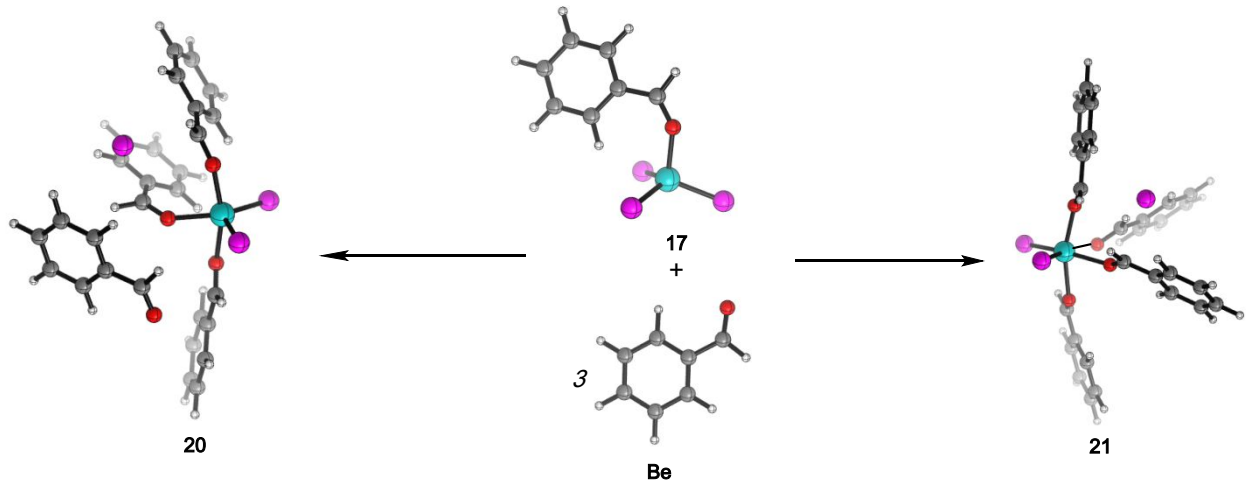

Now we have the following expression for the Gibbs free energy change,

$$\Delta G = \Delta G^0 + RT(lnQ).....(S5) \quad Q = \frac{[20+21]}{[17]\,[Be]^3}$$

Where, Q is reaction quotient and R universal Gas constant, T is temperature.

At equilibrium,

$$\Delta G = \Delta G^0 + RT(lnK_{Eq}).....(S6) \quad K_{Eq} = \frac{[20+21]_{Eq}}{[17]_{Eq}[Be]_{Eq}^3}$$

$$\Delta G^0 = -RT(lnK_{Eq}).....(S7)\,,\ \Delta G = 0, at\ equilibrium$$

Let us assume that at 9.6 equiv (last entry, Table S2) **Be** addition the system attained equilibrium. Then,

$$[20+21]_{Eq} = 8.77 * 10^{-2}\,M$$

$$[17]_{Eq} = 5.62 * 10^{-2}\,M$$

$$[Be]_{Eq} = 7.56 * 10^{-1}\ M$$

$$\Delta G^0 = -\ 0.8\,kcal/mol\ .....\ (S8)\,,\ T = 298.15\,K$$

From Table S2,

$$average\ Q = 2.29 * 10^4$$

Then from eq. 5,

$$\Delta G = \Delta G^0 + RT * ln(2.29 * 10^4)$$

$$\Delta G = 5.2\ kcal/mol,\ T = 298.15\ K$$

Similar to **Ac**, we anticipate that the reaction system will be largely populated by species **21** at superstochiometric **Be** addition, since **21** is 11.1 kcal/mol more stable than **20**. Thus, sound agreement between the experimental results (ΔG = +5.2 kcal/mol) and the theoretically predicted Gibbs free energy (ΔG = +5.8 kcal/mol, Fig 7 right, see in the main manuscript) for the formation of **21** from its precursor gives further evidence that the computational modeling is an accurate representation of the possible solution structures formed in these systems.

S12. Effect of DFT Functional Choice

The energies of key intermediates were evaluated using two additional DFT functionals. Species **16** and **21** are more stable than **15** and **20**, respectively, at all three levels of theory (see below). The consistency in these results indicates that the relative thermodynamic energies of **15**/**16** and **20**/**21** are not strongly dependent on functional.

Table S3. Energetics for select transformations, using three density functionals.

Transformation[a]	ωB97X-D3		M06L-D3		B3LYP-D3	
	ΔG	ΔH	ΔG	ΔH	ΔG	ΔH
11+3Ac→15	17.5	3.9	13.3	-0.2	14.7	1.1
11+3Ac→16	9.8	-3.9	2.5	-11.1	8.9	-4.8
17+3Be→20	15.9	2.5	9.3	-4.1	12.4	-1.0
11+3Be→21	5.8	-7.6	-0.6	-14.1	3.6	-9.8

[a]All values are in kcal/mol and obtained at DFT(Functional)/def2-TZVP/SMD(DCE) level of theory. ΔG values are obtained using 50% scaling of the total entropy.

S13. Effect of Entropy scaling on the computed free energies

The free energies for select transformations were reevaluated by scaling only translational and rotational components of the entropy (see Table S4, S5). The predicted free energy changes are

sensitive to the scaling factor. However, ΔΔG for the two 4:1 complexes remains relatively unaltered with the different scaling, and thus it does not make any qualitative difference in the conclusions.

Table S4: Energetics for select transformations with three entropic scalings.

Selected Transformation	[a]ΔG (No scaling of total Entropy)	[a]ΔG (50% scaling of total entropy)	[a]ΔG (50% scaling of only translational and rotational entropy)
Fc+Ac→11	-19.8	-25.8	-28.8
11+Ac→12	4.0	-2.4	-5.2
11+2Ac→14	30.2	16.9	12.0
11+3Ac→15	36.7	17.5	8.8
11+3Ac→16	29.1	9.8	1.9

[a]All values are in kcal/mol and obtained at ωB97X-D3/def2-TZVP/SMD(DCE) level of theory.

Table S5: Energetics for select transformations, using different scaling of entropy.

Selected Transformation	[a]ΔG (No scaling of total Entropy)	[a]ΔG (50% scaling of total entropy)	[a]ΔG (50% scaling of only translational and rotational entropy)
Fc+Be→17	-15.6	-21.8	-25.2
11+Be→18	0.6	-5.4	-10.8
11+2Be→19	22.3	9.8	0.5
11+3Be→20	35.0	15.9	5.4
11+3Be→21	25.0	5.8	-7.0

[a]All values are in kcal/mol and obtained at ωB97X-D3/def2-TZVP/SMD(DCE) level of theory.

S14. Reason for not observing complex 12 in the experiment.

Based on the computed energetics, species **12** (2:1 complex) is indeed likely to be more populated than species **16** (4:1 complex). Though **12** is more stable than **16**, the relative equilibrium concentration of **12** vs **16** will be dictated by the concentration of carbonyl added into the system. Following Le Chatelier's principle, the equilibrium will shift in the forward direction i.e there

would be a significant population of 4:1 complex in the reaction mixture. This is further supported by the fact of isolation of the crystal structure of the 4:1 benzaldehyde complex in the experiment.[21]

Though the predicted free energies indicate that there should be **12** present in the reaction mixture, its discrete identification in the experiments is challenging as there is a significant overlap between theoretically simulated peaks of **12** (1673 and 1679 cm^{-1}) and **15**+**16** (1657, 1659, 1660, 1666, 1675, and 1679 cm^{-1}). Additionally, in titration experiments, consumption behavior is consistent with three **Ac** consuming one **11**, as well as three **Be** consuming one **17**. In both systems, we see lines of constant slope after the 1 equiv transition. If the system were transitioning from 1:1 to 2:1 and then 4:1, those transitions suggest that there should be more than one change in slope, which is not born out by the data. If this 1:1 to 4:1 transition is occurring, one should see 1) a single change in slope and 2) ionization (conductance) once we pass the one equiv threshold, which is borne out by observations. The spectral overlap between **12** and **15**+**16** therefore shows why **12** is not experimentally isolated, and the titration slopes indicate that the 4:1 complex is more important to the overall interpretation of the spectroscopic results.

S15. Solid State IR Spectroscopy

In a glove box, $FeCl_3$ (50 mg, 0.31 mmol) was added to a scintillation vial equipped with a rice stir bar. Anhydrous DCE (0.24 mL, 1.28 M) followed by anhydrous benzaldehyde (0.16 mL, 1.5 mmol) were added to the vial. The vial was sealed and allowed to stir at room temperature in the glove box for 15 minutes. After 15 minutes the vial was unsealed and placed inside a larger scintillation vial that contained 2 mL pentane. The diffusion chamber was sealed and taken out of the glove box and placed in a freezer until orange crystals were observed (~48 hours). Mother liquor was then removed under reduced pressure and resulting orange crystals were analyzed via

ATR-FTIR. IR Spectra were plotted using Prism GraphPad Pro and are compared to the simulated spectrum for **21**.

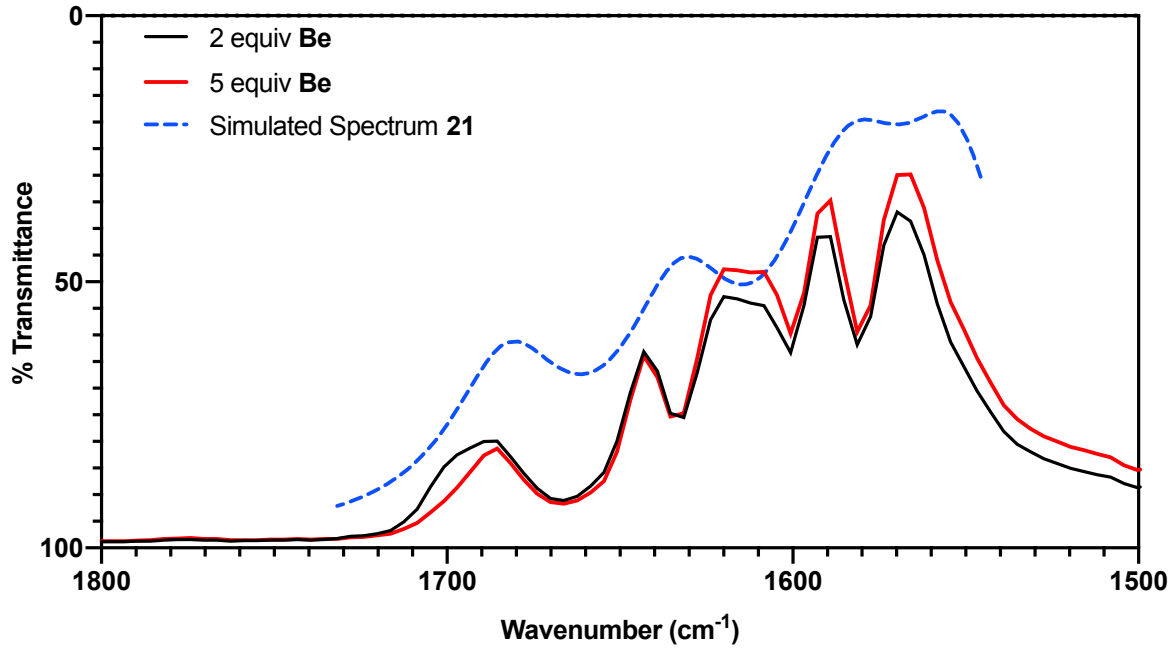

Figure S2: Solid state IR spectra of 4:1 Be:Fc complex **21**.

S16. Deconvolution Analysis

Deconvolution analysis of the IR spectra of beyond 1 equiv carbonyl added to a mixture of $FeCl_3$ in DCE was performed. For each concentration of carbonyl added the simulated vibrations were calculated by a Gaussian line shape, Eq. S9.

$$A = A_{max}^{\left[\frac{(v - v_{max})^2}{\sigma^2}\right]} \tag{S9}$$

Where, A is the absorbance, A_{max} is the band maximum, $\boldsymbol{\nu}$ is the experimental wavenumber, $\boldsymbol{\nu}_{max}$ is the calculated wavenumber of the band maximum, and σ is an adjustable parameter for bandwidth. Initially, a set of A_{max}, $\boldsymbol{\nu}_{max}$, and σ values were used to approximate the band shape as initial guesses for the deconvolution analysis. The simulated vibrations were then calculated using

Solver in Microsoft Excel to minimize the sum of squares of residuals. Spectra were plotted using Prism GraphPad Pro.

$FeCl_3$-Acetone System:

Table S6: Spectral deconvolution data calculated with Eq. S9 used in Figure 9A.

Parameter	Band I	Band II	Band III	Band IV
ν_{max}	1714.80	1691.03	1663.17	1634.35
A_{max}	0.07	0.05	0.07	0.13
σ	11.72	15.55	20.73	26.71

Table S7: Spectral deconvolution data calculated with Eq. S9 used in Figure 9B.

Parameter	Band I	Band II	Band III	Band IV
ν_{max}	1714.44	1691.83	1664.00	1633.73
A_{max}	0.10	0.06	0.09	0.12
σ	10.54	14.60	19.46	26.10

Table S8: Spectral deconvolution data calculated with Eq. S9 used in Figure 9C.

Parameter	Band I	Band II	Band III	Band IV
ν_{max}	1714.25	1692.72	1664.36	1632.79
A_{max}	0.12	0.07	0.12	0.11
σ	9.84	14.14	18.97	25.54

Table S9: Spectral deconvolution data calculated with Eq. S9 used in Figure 9D.

Parameter	Band I	Band II	Band III	Band IV
ν_{max}	1714.12	1692.85	1664.58	1632.56
A_{max}	0.15	0.08	0.13	0.11
σ	9.61	13.85	18.06	25.28

Table S10: Spectral deconvolution data calculated with Eq. S9 used in Figure 9E.

Parameter	Band I	Band II	Band III	Band IV
$\boldsymbol{\nu}_{\mathrm{max}}$	1713.89	1693.04	1665.72	1634.32
$\mathbf{A_{max}}$	0.24	0.10	0.15	0.10
$\boldsymbol{\sigma}$	9.28	13.55	16.02	28.16

Table S11: Average of calculated $\boldsymbol{\nu}_{\mathrm{max}}$ in Tables S3-S7.

Band	Average $\boldsymbol{\nu}_{\mathrm{max}}$
I	1714.3 ± 0.3
II	1692.3 ± 0.8
III	1664.4 ± 0.9
IV	1633.6 ± 0.8

$FeCl_3$-Benzaldehyde System:

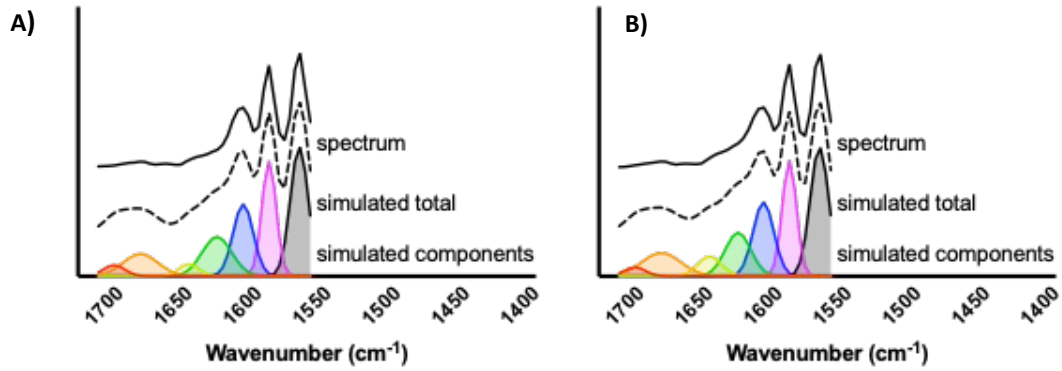

Figure S3: Experimental spectrum (solid black), the spectrum that results from combination of simulated peaks (dashed black), and the simulated vibrations 1704 cm^{-1} (red), 1685 cm^{-1} (orange), 1650 cm^{-1} (yellow), 1629 cm^{-1} (green), 1611 cm^{-1} (blue), 1594 cm^{-1} (violet), and 1574 cm^{-1} (black). A) [**Be**] = 0.161 M, B) [**Be**] = 0.177 M.

Table S12: Spectral deconvolution data calculated with Eq. S9 used in Figure S9A.

Parameter	Band I	Band II	Band III	Band IV	Band V	Band VI	Band VII
ν_{max}	1704.00	1685.00	1650.00	1629.93	1610.97	1592.32	1570.46
A_{max}	0.03	0.05	0.03	0.09	0.16	0.26	0.29
σ	11.00	18.00	10.00	15.05	10.23	7.20	9.12

Table S13: Spectral deconvolution data calculated with Eq. S9 used in Figure S9B.

Parameter	Band I	Band II	Band III	Band IV	Band V	Band VI	Band VII
ν_{max}	1704.00	1685.00	1650.00	1629.60	1611.20	1592.47	1570.70
A_{max}	0.02	0.05	0.04	0.10	0.17	0.26	0.29
σ	11.00	20.00	12.00	13.07	10.59	7.19	9.45

Table S14: Spectral deconvolution data calculated with Eq. S9 used in Figure 9F.

Parameter	Band I	Band II	Band III	Band IV	Band V	Band VI	Band VII
$\boldsymbol{\nu}_{\max}$	1704.00	1685.00	1649.95	1629.97	1611.83	1593.16	1571.84
$\mathbf{A_{max}}$	0.03	0.06	0.08	0.13	0.16	0.26	0.28
$\boldsymbol{\sigma}$	11.00	20.00	10.00	12.04	12.24	6.88	10.87

Table S15: Spectral deconvolution data calculated with Eq. S9 used in Figure 9G.

Parameter	Band I	Band II	Band III	Band IV	Band V	Band VI	Band VII
$\boldsymbol{\nu}_{\max}$	1704.00	1685.00	1649.95	1628.95	1611.61	1593.96	1573.15
$\mathbf{A_{max}}$	0.06	0.07	0.10	0.16	0.15	0.25	0.26
$\boldsymbol{\sigma}$	10.00	15.00	14.00	12.08	12.70	6.53	11.73

Table S16: Spectral deconvolution data calculated with Eq. S9 used in Figure 9H.

Parameter	Band I	Band II	Band III	Band IV	Band V	Band VI	Band VII
$\boldsymbol{\nu}_{\max}$	1704.00	1685.00	1649.95	1628.94	1611.59	1594.52	1574.21
$\mathbf{A_{max}}$	0.08	0.08	0.11	0.20	0.14	0.25	0.26
$\boldsymbol{\sigma}$	10.00	14.00	13.00	12.08	12.72	6.31	12.00

Table S17: Spectral deconvolution data calculated with Eq. S9 used in Figure 9I.

Parameter	Band I	Band II	Band III	Band IV	Band V	Band VI	Band VII
$\boldsymbol{\nu}_{\max}$	1704.00	1685.00	1649.95	1628.96	1611.49	1595.55	1576.46
$\mathbf{A_{max}}$	0.23	0.11	0.14	0.25	0.14	0.27	0.26
$\boldsymbol{\sigma}$	10.00	14.00	13.00	12.00	12.77	6.09	11.96

Table S18: Spectral deconvolution data calculated with Eq. S9 used in Figure 9J.

Parameter	Band I	Band II	Band III	Band IV	Band V	Band VI	Band VII
$\boldsymbol{\nu}_{\max}$	1704.00	1685.00	1649.96	1629.24	1610.75	1596.02	1577.45
$\mathbf{A_{max}}$	0.40	0.14	0.19	0.29	0.15	0.27	0.28
$\boldsymbol{\sigma}$	10.00	15.00	11.08	12.24	12.82	5.97	13.11

Table S19: Average of calculated $\boldsymbol{\nu}_{\max}$ in Tables S9-S15:.

Band	Average $\boldsymbol{\nu}_{\max}$
I	1704 ± 0
II	1685 ± 0
III	1649.97 ± 0.03
IV	1629.5 ± 0.5
V	1611.3 ± 0.4
VI	1594 ± 2
VII	1574 ± 3

S17. Analytical model for Active Catalyst Concentration

To elucidate how activity varies with carbonyl byproduct formation, we fit an analytical model to experimental data under the assumption that metathesis reactivity terminates when 99% of catalyst is consumed. This model is based on the equilibrium between the complex 1:1 complex, carbonyl and 4:1 complex. Thus, we have,

$$\text{1:1 complex} + \mathbf{3}\ \text{carbonyl} \rightleftharpoons \text{4:1 complex}$$

$$K_{Eq} = \frac{[\text{4:1 complex}]}{[\text{1:1 complex}][\text{carbonyl}]^3} \qquad \text{(S10)}$$

For a given catalyst loading, we solve eq S10 numerically, and then plotted [1:1 complex] vs conversion. We hypothesize that it is the [1:1 complex] which is crucial for the carbonyl exchange to carry out successive catalytic cycles. Thus, [1:1 complex] essentially dictates the concentration of the active catalyst present at any time in the reaction medium. Below is a Mathematica code for solving eq. S10.

```
Clear[K_Eq]; Clear[K_Eq]; Clear[F]; Clear[F2]
K_Eq = 0.00063;
F0 = 1; (* relative amount of Fe, initial *)
L1 = 20; (* substrate to Fe ratio, initial *)
L2 = 100; (* substrate to Fe ratio, initial *)
(* x is the amount of 4:1 complex *)
(* c is the conversion 0→1 *)
F[x_, c_] = K_Eq *(F0 - x)*(L1*c - 3 x)^3 - x
F2[x_, c_] = K_Eq *(F0 - x)*(L2*c - 3 x)^3 - x
Plot[{1 - x /. First@NSolve[F[x, c] == 0 && x > 0, x],
  1 - x /. First@NSolve[F2[x, c] == 0 && x > 0, x]}, {c, 0.0, 1}]
```

Note: The value of K_{Eq}=K_{Ac} obtained by fitting experimental results. The same is true for K_{Be}.

S18. Mulliken charge analysis of the species 16 and 21

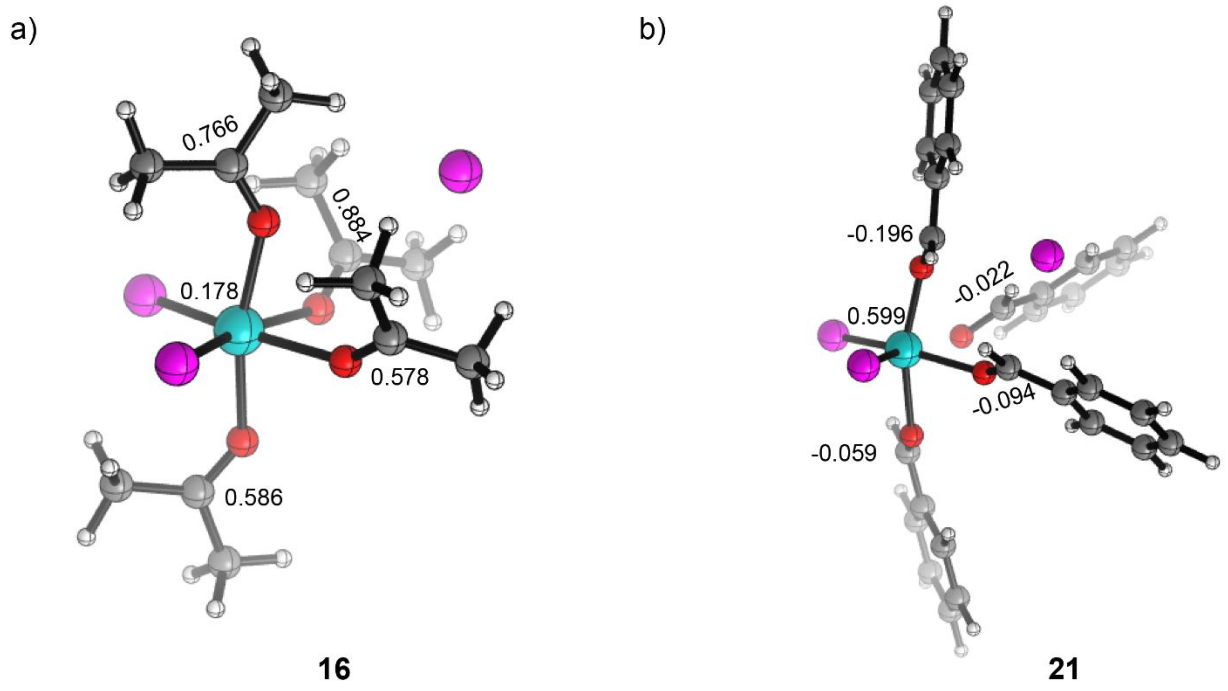

Figure S4: Mulliken charge analysis of complex a) **16**, b) **21**. Color code: Fe cyan, Cl magenta, O red, C grey, H white respectively.

S19. Theoretically predicted C=O stretching vibrations of the Be:Fe 4:2 Lewis pair (with the $FeCl_4^-$ counter anion)

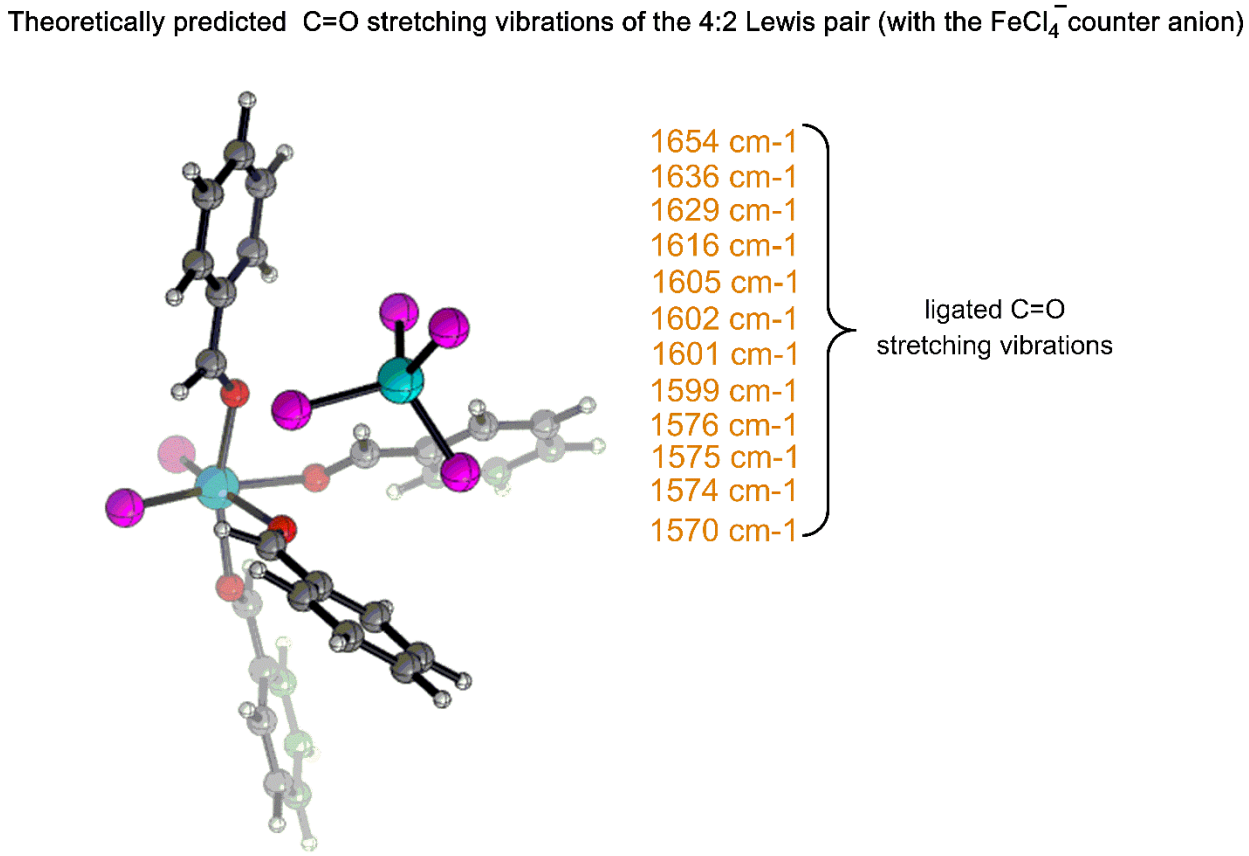

Figure S5: Theoretically predicted C=O IR stretching frequency (cm^{-1}) of the Be:Fe 4:2 Lewis pair (with the $FeCl4^-$ counter anion). Color code: Fe cyan, Cl magenta, O red, C grey, H white respectively.

S20. Table of solvent phase energies and free energies for all the species investigated

Table S20. Solvent phase energies (E_l) for all species investigated. E_l were obtained at ωB97X-D/6-311++G**/CPCM (Benzene) level of theory. Thermal correction to free energies (G_{Corr}) and enthalpies (H_{Corr}) were obtained at B-97D/6-31+G* level of theory at 1 atm pressure and 298.15 K.

Species	E_l in Hartree	G_{corr} in Hartree	H_{corr} in Hartree
Fc	-2644.517934	-0.029220143	0.010348839
Ac	-193.1850924	0.053654358	0.087901388
11	-2837.75299	0.045874821	0.100607162
12	-3030.951713	0.122571633	0.191074246
TS1	-3030.918192	0.121582729	0.189893388
13	-3030.922798	0.125462048	0.191310099
14	-3224.116627	0.200794824	0.281813836
15	-3417.309735	0.275922635	0.372005227
16	-3417.321765	0.275791444	0.371662603
Be	-345.6057659	0.076351685	0.114399771
17	-2990.168245	0.069822368	0.127566095
18	-3335.791579	0.167655609	0.244337142
19	-3681.382791	0.267057559	0.361079505
20	-4026.988217	0.366449342	0.477405938
21	-4027.005751	0.368018927	0.478803525

S21. References

(1) Shao, Y.; Gan, Z.; Epifanovsky, E.; Gilbert, A. T. B.; Wormit, M.; Kussmann, J.; Lange, A. W.; Behn, A.; Deng, J.; Feng, X.; Ghosh, D.; Goldey, M.; Horn, P. R.; Jacobson, L. D.; Kaliman, I.; Khaliullin, R. Z.; Kuś, T.; Landau, A.; Liu, J.; Proynov, E. I.; Rhee, Y. M.; Richard, R. M.; Rohrdanz, M. A.; Steele, R. P.; Sundstrom, E. J.; Woodcock, H. L.; Zimmerman, P. M.; Zuev, D.; Albrecht, B.; Alguire, E.; Austin, B.; Beran, G. J. O.; Bernard, Y. A.; Berquist, E.; Brandhorst, K.; Bravaya, K. B.; Brown, S. T.; Casanova, D.; Chang, C.-M.; Chen, Y.; Chien, S. H.; Closser, K. D.; Crittenden, D. L.; Diedenhofen, M.; DiStasio, R. A.; Do, H.; Dutoi, A. D.; Edgar, R. G.; Fatehi, S.; Fusti-Molnar, L.; Ghysels, A.; Golubeva-Zadorozhnaya, A.; Gomes, J.; Hanson-Heine, M. W. D.; Harbach, P. H. P.; Hauser, A. W.; Hohenstein, E. G.; Holden, Z. C.; Jagau, T.-C.; Ji, H.; Kaduk, B.; Khistyaev,

K.; Kim, J.; Kim, J.; King, R. A.; Klunzinger, P.; Kosenkov, D.; Kowalczyk, T.; Krauter, C. M.; Lao, K. U.; Laurent, A. D.; Lawler, K. V.; Levchenko, S. V.; Lin, C. Y.; Liu, F.; Livshits, E.; Lochan, R. C.; Luenser, A.; Manohar, P.; Manzer, S. F.; Mao, S.-P.; Mardirossian, N.; Marenich, A. V.; Maurer, S. A.; Mayhall, N. J.; Neuscamman, E.; Oana, C. M.; Olivares-Amaya, R.; O'Neill, D. P.; Parkhill, J. A.; Perrine, T. M.; Peverati, R.; Prociuk, A.; Rehn, D. R.; Rosta, E.; Russ, N. J.; Sharada, S. M.; Sharma, S.; Small, D. W.; Sodt, A.; Stein, T.; Stück, D.; Su, Y.-C.; Thom, A. J. W.; Tsuchimochi, T.; Vanovschi, V.; Vogt, L.; Vydrov, O.; Wang, T.; Watson, M. A.; Wenzel, J.; White, A.; Williams, C. F.; Yang, J.; Yeganeh, S.; Yost, S. R.; You, Z.-Q.; Zhang, I. Y.; Zhang, X.; Zhao, Y.; Brooks, B. R.; Chan, G. K. L.; Chipman, D. M.; Cramer, C. J.; Goddard, W. A.; Gordon, M. S.; Hehre, W. J.; Klamt, A.; Schaefer, H. F.; Schmidt, M. W.; Sherrill, C. D.; Truhlar, D. G.; Warshel, A.; Xu, X.; Aspuru-Guzik, A.; Baer, R.; Bell, A. T.; Besley, N. A.; Chai, J.-D.; Dreuw, A.; Dunietz, B. D.; Furlani, T. R.; Gwaltney, S. R.; Hsu, C.-P.; Jung, Y.; Kong, J.; Lambrecht, D. S.; Liang, W.; Ochsenfeld, C.; Rassolov, V. A.; Slipchenko, L. V.; Subotnik, J. E.; Van Voorhis, T.; Herbert, J. M.; Krylov, A. I.; Gill, P. M. W.; Head-Gordon, M. Advances in Molecular Quantum Chemistry Contained in the Q-Chem 4 Program Package. *Mol. Phys.* **2015**, *113* (2), 184–215. https://doi.org/10.1080/00268976.2014.952696.

(2) Grimme, S. Semiempirical GGA-Type Density Functional Constructed with a Long-Range Dispersion Correction. *J. Comput. Chem.* **2006**, *27* (15), 1787–1799. https://doi.org/10.1002/jcc.20495.

(3) Zimmerman, P. M. Automated Discovery of Chemically Reasonable Elementary Reaction Steps. *J. Comput. Chem.* **2013**, *34* (16), 1385–1392. https://doi.org/10.1002/jcc.23271.

(4) Zimmerman, P. M. Navigating Molecular Space for Reaction Mechanisms: An Efficient,

Automated Procedure. *Mol Simul* **2014**, *41* (1–3), 43–54. https://doi.org/10.1080/08927022.2014.894999.

(5) Zimmerman, P. M. Growing String Method with Interpolation and Optimization in Internal Coordinates: Method and Examples. *J. Chem. Phys.* **2013**, *138* (18), 184102. https://doi.org/10.1063/1.4804162.

(6) Marenich, A. V.; Olson, R. M.; Kelly, C. P.; Cramer, C. J.; Truhlar, D. G. Self-Consistent Reaction Field Model for Aqueous and Nonaqueous Solutions Based on Accurate Polarized Partial Charges. *J. Chem. Theory Comput.* **2007**, *3* (6), 2011–2033. https://doi.org/10.1021/ct7001418.

(7) Lin, Y.-S.; Li, G.-D.; Mao, S.-P.; Chai, J.-D. Long-Range Corrected Hybrid Density Functionals with Improved Dispersion Corrections. *J. Chem. Theory Comput.***2013**, *9* (1), 263–272. https://doi.org/10.1021/ct300715s.

(8) Neese, F. The ORCA Program System. *WIREs Comput. Mol. Sci.* **2012**, *2* (1), 73–78. https://doi.org/10.1002/wcms.81.

(9) Contreras-García, J.; Johnson, E. R.; Keinan, S.; Chaudret, R.; Piquemal, J.-P.; Beratan, D. N.; Yang, W. NCIPLOT: A Program for Plotting Noncovalent Interaction Regions. *J. Chem. Theory Comput.* **2011**, *7* (3), 625–632. https://doi.org/10.1021/ct100641a.

(10) Wertz, D. H., Relationship between the gas-phase entropies of molecules and their entropies of solvation in water and 1-octanol. *J. Am. Chem. Soc* **1980**, *102* (16), 5316-5322. https://pubs.acs.org/doi/10.1021/ja00536a033

(11) Spickermann, C. Entropies of Condensed Phases and Complex Systems, Springer Theses,

2010, Chap. 3, pp. 76–80, and references therein

(12) Plata, R. E.; Singleton, D. A., A Case Study of the Mechanism of Alcohol-Mediated Morita Baylis–Hillman Reactions. The Importance of Experimental Observations. *J. Am. Chem. Soc* **2015,** *137* (11), 3811-3826. https://pubs.acs.org/doi/10.1021/ja5111392

(13) Jensen, J. H. Predicting accurate absolute binding energies in aqueous solution: thermodynamic considerations for electronic structure methods. Phys. Chem. Chem. Phys. **2015**, *17* (19), 12441-12451. https://doi.org/10.1039/C5CP00628G.

(14) Hanson, C. S.; Psaltakis, M. C.; Cortes, J. J.; Siddiqi, S. S.; Devery, J. J., Investigation of Lewis Acid-Carbonyl Solution Interactions via Infrared-Monitored Titration. *J. Org. Chem* **2020**, *85* (2), 820-832. https://pubs.acs.org/doi/10.1021/acs.joc.9b02822

(15) Susz, B. P.; Cooke, I., Etude du spectre infrarouge de complexes formés par les halogénures d'aluminium. I. Complexes de l'acétophénone et de la benzophénone; comparaison avec les spectres de divers compossé organiques présentant la liaison aluminium-oxygène. *Helv. Chim. Acta* **1954**, *37* (4), 1273-1280. https://doi//10.1002/hlca.19540370432

(16) Susz, B. P.; Chalandon, P., Etude de composés d'addition des acides de Lewis. IX. — Spectres d'absorption infrarouge des composés formés par la benzophénone et l'acétophénone avec BF_3, $FeCl_3$, $ZnCl_2$ et $AlCl_3$ et nature de la liaison oxygène-métal. *Helv. Chim. Acta* **1958**, *41* (5), 1332-1341. https://doi/10.1002/hlca.19580410519

(17) Chalandon, P.; Susz, B. P., Etude de composés d'addition des acides de Lewis. VI Spectre d'absorption infrarouge de l'acétone-trifluorure de bore; spectre d'absorption infrarouge et moment de dipŏle du di-propyl-cétone-trifluorure de bore. *Helv. Chim. Acta* **1958**, 41 (3), 697-704. https://doi/10.1002/hlca.660410316

(18) Greenwood, N. N., The ionic properties and thermochemistry of addition compounds of gallium trichloride and tribromide. *J. Inorg. Nucl. Chem.* **1958**, *8*, 234-240. https://doi.org/10.1016/0022-1902(58)80186-4

(19) Greenwood, N. N.; Perkins, P. G., 68. Thermochemistry of the systems which boron trichloride and gallium trichloride form with acetone and acetyl chloride, and the heat of solution of boron tribromide in acetone *J. Chem. Soc* **1960**, (0), 356-360. https://doi.org/10.1039/JR9600000356

(20) Davlieva, M. G.; Lindeman, S. V.; Neretin, I. S.; Kochi, J. K., Isolation, X-ray Structures, and Electronic Spectra of Reactive Intermediates in Friedel−Crafts Acylations. *J. Org. Chem* **2005**, *70* (10), 4013-4021. https://doi.org/10.1021/jo0501588

(21) Hanson, C. S.; Psaltakis, M. C.; Cortes, J. J.; Devery, J. J., Catalyst Behavior in Metal-Catalyzed Carbonyl-Olefin Metathesis. *J. Am. Chem. Soc* **2019**, *141* (30), 11870-11880. https://doi.org/10.1021/jacs.9b02613

(22) Wiberg, K. B., Application of the pople-santry-segal CNDO method to the cyclopropylcarbinyl and cyclobutyl cation and to bicyclobutane. *Tetrahedron* **1968**, *24* (3), 1083-1096. https://doi.org/10.1016/0040-4020(68)88057-3

S22. Cartesian coordinates of all species investigated

Fc

Fe	-0.99144245	-0.17139218	0.00319325
Cl	-2.06265593	1.69003656	-0.01195794
Cl	-0.53736920	-1.13671235	1.86546125
Cl	-0.54433242	-1.16101203	-1.84814655

Ac

O	-3.93716596	3.11184047	-1.29559041
C	-3.94059985	4.32503811	-1.12691593
C	-2.89172434	5.02778346	-0.26707448
C	-4.99589986	5.22825922	-1.76207210
H	-5.67522443	5.59909080	-0.97372293
H	-4.52847275	6.11447423	-2.22420532
H	-5.57850331	4.67089207	-2.50805197
H	-2.23347882	5.63024423	-0.91837075
H	-3.37074640	5.72831180	0.43821406
H	-2.28645249	4.29117556	0.27856643

11

Fe	-0.72187475	0.00210842	0.00089514
Cl	-2.16075525	1.63082192	-0.01507444
Cl	-0.64413739	-1.16901425	1.85697106
Cl	-0.65794423	-1.21974623	-1.82242257
O	1.11069629	0.90383537	-0.01004010
C	2.26993814	0.43533240	-0.00657505
C	3.43899573	1.37940317	-0.00264405
H	4.06304333	1.17228292	0.88437010
H	4.07073155	1.17177166	-0.88401371
H	3.10829088	2.42527642	-0.00418355
C	2.51239779	-1.04672535	-0.00503363
H	3.58238038	-1.29293673	-0.00371426
H	2.01636328	-1.48808337	0.87636471
H	2.01762823	-1.48976036	-0.88625162

12

Fe	-0.09163881	-0.12993501	0.67151056
Cl	-1.95569732	-0.56471182	1.85975330
Cl	-0.03914874	-0.53775455	-1.51237212
O	-0.83238816	1.89565099	0.27439410
C	-1.12244807	2.87208747	0.98250986
O	0.61579040	-2.16462940	1.11320781
C	0.21120947	-3.30370559	0.83532356
Cl	1.74501964	0.68800697	1.62588827
C	-1.62320723	4.13647204	0.32531104
H	-2.61430522	4.39181790	0.73920527
H	-0.94812287	4.97061341	0.58520200
H	-1.68220859	4.01882845	-0.76405211
C	0.98183651	-4.50206096	1.33826140
H	1.22580058	-5.16626664	0.49132639
H	1.89524880	-4.19231438	1.86176640
H	0.33260314	-5.08170380	2.01823602
C	-1.02189606	-3.54543050	0.00114220
H	-1.32191517	-4.60282369	0.01397259
H	-1.84250171	-2.90334032	0.35469198
H	-0.80263641	-3.23673032	-1.03560601
C	-0.99717951	2.84523439	2.48529234
H	0.04322102	2.60117480	2.75516607
H	-1.29377540	3.80097513	2.93934795
H	-1.62240091	2.02692179	2.87822670

TS1

Fe	1.57159799	1.42102451	0.68759848
Cl	2.75652795	1.79219030	-1.12997730
Cl	2.90457803	1.51904920	2.45101794
O	0.38111941	2.88209516	1.09499349
C	-0.61472663	3.22717355	0.35438125
O	1.15632853	-0.56730857	0.95877265
C	1.10326414	-1.59423579	0.25436614
Cl	-0.90980591	1.04955879	-0.75938464
C	-1.96391996	3.34561164	1.02192442
H	-1.98299701	4.32400977	1.53843384
H	-2.77347963	3.32020251	0.28113793
H	-2.09806991	2.55029107	1.76538700
C	0.58006036	-2.86726271	0.86263350
H	1.35473581	-3.65011389	0.79136504
H	0.28243087	-2.71641200	1.90760647
H	-0.27958436	-3.21647554	0.26398132
C	-0.34370008	4.05264732	-0.88174255
H	-1.19450777	4.02564441	-1.57425210
H	-0.19594846	5.09387418	-0.53617737
H	0.57091397	3.71542641	-1.38450516
C	1.50733185	-1.59023490	-1.19181463
H	2.43973282	-1.02396419	-1.33210722
H	1.59939293	-2.60839124	-1.59423371
H	0.72365524	-1.04268933	-1.74689841

13

Fe	-1.02051730	-0.21577416	0.16057858
Cl	-1.74023042	-1.34084423	1.90806598
Cl	-1.92360371	-0.82255251	-1.73458888
O	-1.04452575	1.61170149	0.34679892
C	-0.88937319	2.56205158	1.28243261
O	0.96838946	-0.45239605	-0.04224174
C	1.99021795	-0.49682319	0.67376477
Cl	0.95488430	2.29751275	2.13134548
C	-0.80727355	3.95444846	0.66183237
H	-1.79416052	4.17977423	0.22278120
H	-0.56595540	4.70823529	1.42352727
H	-0.05106625	3.97225536	-0.13418051
C	3.29420955	-0.00980118	0.10420751
H	4.13444225	-0.63778781	0.43858899
H	3.25002874	0.05073571	-0.99074879

H	3.45550004	1.00457226	0.51254958
C	1.98065749	-1.03188238	2.07637020
H	2.49199502	-2.01245893	2.06254868
H	2.56617847	-0.36751645	2.73006700
H	0.96350896	-1.15541759	2.46376184
C	-1.84523255	2.42753067	2.46532422
H	-2.87044014	2.56331142	2.08047096
H	-1.76286108	1.42935594	2.91430517
H	-1.63583898	3.19449574	3.22349597

14

Fe	-1.21117452	-0.18364303	0.01648179
Cl	-2.46513065	-0.76836084	1.79774067
Cl	-2.23755831	-0.09822990	-1.95364898
O	-0.89599102	1.61833166	0.41053167
C	-0.63256763	2.56694452	1.28773785
O	0.85078774	-0.33244685	-0.23149057
C	1.76026415	-0.47849769	0.60304919
O	-0.77751204	-2.44028635	-0.19939118
C	-1.49716389	-3.43025975	-0.39592779
Cl	1.48867499	2.64699648	1.53090100
C	-0.93055451	3.96442265	0.75108466
H	-2.02732572	4.05123528	0.65588339
H	-0.56083429	4.73625677	1.43929666
H	-0.47561848	4.09450172	-0.23934692
C	3.19286769	-0.29685478	0.17383217
H	3.82222763	-1.11251246	0.56478507
H	3.26684671	-0.23178149	-0.91914138
H	3.55259722	0.64699804	0.61875996
C	-0.87121291	-4.80743282	-0.44915907
H	-1.36417772	-5.46454642	0.28822537
H	-1.06108793	-5.25069909	-1.44233873
H	0.20885785	-4.75960945	-0.25858056
C	-1.09133773	2.29886280	2.71766666
H	-2.19282952	2.24217691	2.70769547
H	-0.70413815	1.34022362	3.08266902
H	-0.76626174	3.10897546	3.38436264
C	1.49221439	-0.84367090	2.04005907
H	1.99415588	-1.80020227	2.26688285
H	1.93495935	-0.07014581	2.68680902
H	0.41855794	-0.93281420	2.24964465
C	-2.99114790	-3.32825580	-0.57359590
H	-3.43425576	-4.28575715	-0.88207222
H	-3.43010303	-3.00750071	0.38623397
H	-3.22280902	-2.53735371	-1.30251402

15

Fe	-1.63239311	-0.41991493	0.86467931
O	0.47238258	-0.55254926	-3.30475118
C	0.14240212	0.61073098	-3.06997903
Cl	-1.88653114	-0.70873401	3.05000233
Cl	-3.59943937	-0.46941004	-0.19653207
O	-1.25300349	1.43967781	0.66365022
C	-0.79613784	2.52832950	1.21749360
O	0.27839854	-0.66166445	0.01055174
C	1.44229761	-0.65378072	0.45367235
O	-1.41635370	-2.62280504	0.59249573
C	-1.45125568	-3.38169131	-0.38914033
Cl	1.40201628	2.60394946	0.78334780
C	-1.23158426	3.80460243	0.50887040
H	-2.31278777	3.92884300	0.70038048
H	-0.68878307	4.67701730	0.89483788
H	-1.07137098	3.71455947	-0.57314924
C	-1.30382886	1.00742829	-2.82702034
H	-1.40761117	1.40557047	-1.80376140
H	-1.59612007	1.81644084	-3.51854204
H	-1.97619951	0.14950143	-2.95153242
C	2.59595199	-0.58386443	-0.51142926
H	3.37511446	-1.31213495	-0.23418079
H	2.25721339	-0.73520428	-1.54396879
H	3.03437210	0.42442085	-0.41134526
C	-1.35536958	-4.87489867	-0.17166211
H	-2.23642431	-5.36301392	-0.62360804
H	-0.47288354	-5.26358582	-0.70943190
H	-1.29112942	-5.11797820	0.89672855
C	-0.75769338	2.57614366	2.73682951
H	-1.80345903	2.55740653	3.09093218
H	-0.24385352	1.69996916	3.14853179
H	-0.26542216	3.49459711	3.08190297
C	1.74848152	-0.71381234	1.92532682
H	2.43583130	-1.55376059	2.12316325
H	2.27179880	0.21724735	2.19857785
H	0.83811203	-0.81924034	2.52810918
C	1.16533369	1.72987810	-2.96666131
H	0.84060573	2.61014050	-3.54631704
H	1.23862113	2.05193796	-1.91221771
H	2.14978591	1.38932183	-3.31596643
C	-1.60096307	-2.88013629	-1.80199509
H	-0.89001436	-2.06556855	-2.00979535
H	-1.46383920	-3.68612453	-2.53670045
H	-2.61543589	-2.45903084	-1.90915418

16

Fe	-1.32503368	0.18323500	0.89510129
Cl	-1.20942764	-1.05627543	2.82884346
Cl	-3.35573938	-0.42537259	-0.01429549
O	-2.09154520	1.91362377	1.90338753
C	-3.03978249	2.16377266	2.66487932
C	-4.00920599	1.10820230	3.12536131
H	-3.45398272	0.34909431	3.70129327
H	-4.81850972	1.53194454	3.73643275
H	-4.41648682	0.58235294	2.24750214
C	-3.23324199	3.58071527	3.15104840
H	-2.42438238	4.23334927	2.79845759
H	-3.28725301	3.58755407	4.25309043
H	-4.20737389	3.95191267	2.78608898
Cl	2.56718113	0.33131621	-2.05881283
O	0.59169170	1.07271614	1.33071119

C	1.79046788	0.74587587	1.34623810
C	2.24580062	-0.68777435	1.41862514
H	3.15362849	-0.77273242	2.03539154
H	2.51222415	-0.97613216	0.38607798
H	1.45002019	-1.33517021	1.80451437
C	2.84804396	1.81232727	1.23734756
H	3.28515216	1.70053615	0.22639678
H	3.65032561	1.64997169	1.97454775
H	2.41009235	2.81377038	1.34166763
O	-0.99478218	1.57488853	-0.70948845
C	-0.74246306	1.54959491	-1.92635803
C	-0.97493941	0.33733465	-2.78716626
H	-1.68066123	-0.35415140	-2.31301871
H	-1.32930689	0.63673338	-3.78567228
H	0.01445575	-0.14048383	-2.91090476
C	-0.12129754	2.75792589	-2.57621507
H	-0.63091726	3.00477681	-3.52139086
H	-0.11893941	3.61675184	-1.89212201
H	0.91974352	2.46977766	-2.81702546
O	-0.22899872	-1.17548664	-0.26238773
C	-0.22929504	-2.38643614	-0.54786775
C	0.80405106	-2.91587748	-1.50339472
H	0.28094175	-3.34442191	-2.37817599
H	1.34055749	-3.75497495	-1.02556180
H	1.50196258	-2.12694710	-1.81931992
C	-1.25056761	-3.32597620	0.03521848
H	-2.25524511	-2.98555273	-0.26709152
H	-1.08529605	-4.36409933	-0.28369025
H	-1.22833158	-3.24499089	1.13449892

Be

C	-4.07653586	1.45870207	-0.00007283
O	-2.85305983	1.38126385	-0.00147787
H	-4.70384652	0.53031464	0.00156571
C	-4.85627461	2.72245774	-0.00012491
C	-6.26573745	2.65857595	0.00188814
C	-4.20737072	3.97789447	-0.00209762
C	-7.02554480	3.83802882	0.00189349
H	-6.75740985	1.68155435	0.00339650
C	-4.96631594	5.15382154	-0.00207924
H	-3.11654334	4.00223404	-0.00357566
C	-6.37447837	5.08460883	-0.00006500
H	-8.11636228	3.78939672	0.00340559
H	-4.46928609	6.12617972	-0.00358450
H	-6.96320484	6.00468219	-0.00003736

17

Cl	-2.03087060	1.01534890	-1.67809440
Cl	-3.94346265	1.44449460	1.44320795
Cl	-5.60799096	0.23644920	-1.59179862
O	-4.40515495	3.32020492	-1.22848133
C	-4.16888662	4.51480198	-0.94151110
C	-3.06102000	5.03728221	-0.16463473
C	-3.07491627	6.42794980	0.12510857
C	-1.99473148	4.22738349	0.30611616
C	-2.04874271	6.99757439	0.88371754
H	-3.89688307	7.04572852	-0.24514445
C	-0.96652281	4.80733705	1.05168924
H	-1.95891628	3.16808664	0.06562382
C	-0.99517545	6.18530348	1.34644976
H	-2.06210074	8.06405586	1.11315924
H	-0.14244298	4.18738830	1.40725147
H	-0.18882303	6.62879532	1.93429546
H	-4.89322014	5.26099537	-1.32263347
Fe	-3.97932398	1.41520730	-0.75051839

18

Cl	-2.66856207	0.51911036	-2.19022223
Cl	-3.89404226	2.06588599	1.11797098
Cl	-6.40529652	1.55790920	-1.74880312
O	-4.79675647	-0.65235060	-0.26439979
C	-4.88185815	-1.11362354	0.88523410
O	-3.86156488	3.34046536	-1.78888573
C	-3.40619450	4.36452502	-1.25455355
C	-5.18076383	-2.51814371	1.16529813
C	-5.24091539	-2.94063913	2.51347227
C	-5.40355858	-3.44522230	0.11789628
C	-5.51910092	-4.28004230	2.81548092
H	-5.06786671	-2.21513683	3.31243013
C	-5.68247495	-4.77957089	0.42532524
H	-5.35069552	-3.09683566	-0.91426343
C	-5.74056980	-5.19695015	1.77154284
H	-5.56476101	-4.61021147	3.85475946
H	-5.85470110	-5.50011097	-0.37635871
H	-5.95828878	-6.24127154	2.00521966
H	-4.72187024	-0.44574685	1.75487366
C	-3.07854675	5.57979969	-2.00058614
C	-2.55569843	6.68675029	-1.29278324
C	-3.26672401	5.65408187	-3.40230513
C	-2.22069753	7.86109294	-1.97961765
H	-2.41487940	6.61550722	-0.21133189
C	-2.93134875	6.82843400	-4.08177517
H	-3.67087227	4.78711900	-3.92652487
C	-2.40884473	7.92984258	-3.37200997
H	-1.81523531	8.71745578	-1.43790859
H	-3.07217903	6.89375567	-5.16216153
H	-2.14807218	8.84470500	-3.90857977
H	-3.23182552	4.37820255	-0.16023227
Fe	-4.33241440	1.36172342	-0.98727085

19

Cl	-2.35848385	-0.67207499	1.67947430
Cl	-2.33931351	-0.70176810	-2.15211884
O	-1.53878091	1.74939281	-0.23073215
C	-1.45986611	2.49490403	0.77056735
O	0.59115069	-0.02537003	-0.26133649
C	1.47910278	-0.04706816	0.70242518
H	1.19263654	-0.58144866	1.62005545

O	-0.62487018	-2.49660198	-0.15652305
C	-1.38224716	-3.46289097	-0.33843008
H	-2.45773446	-3.28742220	-0.54251869
Cl	1.42877132	1.89856673	1.69560933
H	-1.53991110	2.05623423	1.77940605
C	-1.31341733	3.94300995	0.67333276
C	-1.26472880	4.69469123	1.86944109
C	-1.21685446	4.59109465	-0.58096462
C	-1.11920708	6.08605025	1.81402768
H	-1.32228801	4.17772646	2.82984382
C	-1.07110184	5.98003055	-0.63037152
H	-1.25253298	3.98994392	-1.49012654
C	-1.02301186	6.72679730	0.56508167
H	-1.07392045	6.66967470	2.73514152
H	-0.99224593	6.48748406	-1.59361785
H	-0.90705870	7.81187409	0.52086848
C	2.90888273	-0.20015131	0.30596754
C	3.86268403	-0.53939341	1.28724466
C	3.30881447	-0.04019222	-1.03550033
C	5.20624327	-0.71881855	0.93131868
H	3.54680536	-0.64002539	2.32832182
C	4.65406085	-0.21923623	-1.38908781
H	2.56006524	0.21701000	-1.78520796
C	5.60485879	-0.55692041	-0.40886495
H	5.94250698	-0.97797544	1.69529054
H	4.96244569	-0.09578294	-2.42964439
H	6.65231226	-0.69323150	-0.68743912
C	-0.93689609	-4.85733123	-0.31213807
C	-1.89209035	-5.87600919	-0.53362632
C	0.42039827	-5.19152580	-0.08507181
C	-1.49707111	-7.22020505	-0.52500932
H	-2.93563443	-5.60434570	-0.71123500
C	0.80950664	-6.53368107	-0.07957714
H	1.14147751	-4.38922908	0.07707493
C	-0.14761961	-7.54672402	-0.29931154
H	-2.23162257	-8.00951972	-0.69418050
H	1.85425073	-6.79920602	0.09205975
H	0.16238919	-8.59388783	-0.29419120
Fe	-1.27539444	-0.33326779	-0.24260728

20

Fe	-2.22159406	-0.40013202	1.04392575
O	-0.60873059	-1.84527621	-2.96374926
C	-0.47956434	-0.63281323	-2.78537670
Cl	-3.04928932	-1.29651190	2.92259075
Cl	-3.69165151	-0.32406279	-0.61537577
O	-2.23707624	1.46678441	1.66840526
C	-1.82353880	2.57111728	2.10704926
O	-0.40436408	0.02920466	0.28479354
C	0.70341242	0.47457346	0.69055191
O	-1.45111146	-2.37133652	0.55206298
C	-1.63497649	-3.06046557	-0.47065552
Cl	0.42511732	3.24315604	0.60384458
C	0.81796326	0.07469872	-2.71639943
C	0.82353455	1.47021454	-2.51224274
C	2.03970493	-0.63310689	-2.79872515
C	2.03940805	2.15955281	-2.39145122
H	-0.12150675	2.00519153	-2.40038617
C	3.25116920	0.05584826	-2.68014043
H	2.01017729	-1.71383326	-2.94808303
C	3.25101623	1.45269257	-2.47670612
H	2.03444329	3.23153027	-2.19374990
H	4.19777947	-0.48612160	-2.73850577
H	4.19903917	1.98577390	-2.37388930
C	-1.19752705	2.74325969	3.41942117
C	-1.11391487	1.67166422	4.33679331
C	-0.69705131	4.01890492	3.76931946
C	-0.52338608	1.87873114	5.58852312
H	-1.52341898	0.69941483	4.06696728
C	-0.10585066	4.21758984	5.02041028
H	-0.73658070	4.82322862	3.03311773
C	-0.01649093	3.14545567	5.93060405
H	-0.45838112	1.05281195	6.29916880
H	0.29289887	5.19823080	5.28723505
H	0.44824638	3.29954400	6.90743562
C	1.21212709	0.28527918	2.05605933
C	2.30216195	1.06862555	2.50067787
C	0.68413892	-0.72411394	2.89220568
C	2.83466898	0.86214334	3.77712565
H	2.67650099	1.86379349	1.85462828
C	1.23077144	-0.93576093	4.16373851
H	-0.12459206	-1.36195283	2.53814437
C	2.29924795	-0.13960507	4.61022264
H	3.65879922	1.48472245	4.13054165
H	0.81824750	-1.71721633	4.80506677
H	2.71715566	-0.29765403	5.60708859
C	-0.92950932	-4.31457392	-0.72294418
C	-1.14981020	-4.96766476	-1.95700228
C	-0.03058901	-4.86333289	0.22343373
C	-0.47611547	-6.16133676	-2.24491796
H	-1.82303316	-4.51446522	-2.68682026
C	0.63570353	-6.05669119	-0.06748619
H	0.12424432	-4.34372202	1.16998332
C	0.41600539	-6.70312431	-1.30193280
H	-0.63577081	-6.66349750	-3.20068166
H	1.32800147	-6.48807114	0.65816199
H	0.94499790	-7.63182392	-1.52723377
H	-2.10247336	3.47733103	1.54989934
H	1.39696010	0.85558120	-0.06841289
H	-1.37638659	0.01416969	-2.64814032
H	-2.35444752	-2.72337331	-1.23624886

21

Fe	-1.43509589	-0.60779976	0.52676514
O	-1.24230224	-0.67255878	-1.80198926
C	-0.51449591	0.20005793	-2.31013532
H	0.01869367	0.92184577	-1.66608159
Cl	-1.13146670	-0.46820745	2.75546165

Cl	-3.64212548	-0.99273411	0.24174819
O	-1.52002172	1.38893274	0.15543163
C	-1.00898663	2.38253557	0.74082693
O	0.66412253	-0.61862642	0.15961203
C	1.62070506	-0.05955210	0.74557480
H	1.44195966	0.51967140	1.66464999
O	-0.96547746	-2.72440208	0.30752567
C	-1.48315945	-3.50109798	-0.51173058
H	-2.37088369	-3.17535898	-1.08724857
Cl	1.59389155	2.54455265	-0.27763462
H	-0.41754502	2.22758796	1.65496717
C	-0.28785321	0.36393065	-3.74810107
C	0.61224190	1.38207899	-4.14239364
C	-0.93205486	-0.43886217	-4.71886748
C	0.86914933	1.59299230	-5.50419690
H	1.09664631	1.98855390	-3.37159159
C	-0.67322197	-0.22051308	-6.07510018
H	-1.62961700	-1.21091096	-4.38973889
C	0.22669565	0.79389142	-6.46686087
H	1.56362355	2.37569811	-5.81511717
H	-1.16824726	-0.83072052	-6.83354237
H	0.42322118	0.96040719	-7.52845214
C	-1.36773204	3.75452028	0.37814895
C	-0.78104698	4.82317570	1.09181695
C	-2.31484053	4.01535459	-0.63832356
C	-1.13025857	6.14282543	0.78578577
H	-0.03327291	4.60541947	1.85667714
C	-2.66135794	5.33711650	-0.94016939
H	-2.76987012	3.17659792	-1.16667816
C	-2.06927542	6.40055361	-0.23138046
H	-0.67037296	6.97052899	1.32912304
H	-3.39403420	5.54368441	-1.72303809
H	-2.34041471	7.43114844	-0.47125741
C	3.01663620	-0.32690290	0.37085925
C	4.05392443	0.28488585	1.10670228
C	3.32741226	-1.21533257	-0.68277343
C	5.39080748	0.01574616	0.78963688
H	3.79959947	0.98760592	1.90269503
C	4.66460828	-1.48176946	-0.99792373
H	2.51189582	-1.68408332	-1.23548498
C	5.69719917	-0.86638202	-0.26355801
H	6.19382062	0.49561179	1.35264666
H	4.90767089	-2.16616807	-1.81371420
H	6.74033267	-1.07315481	-0.51337580
C	-0.96682617	-4.84786420	-0.76452521
C	-1.62611865	-5.66443291	-1.71173600
C	0.17954861	-5.32810502	-0.08583231
C	-1.14706340	-6.95461866	-1.97670977
H	-2.50758688	-5.28058445	-2.23160966
C	0.65382168	-6.61480769	-0.35484876
H	0.67295467	-4.67862139	0.63848532
C	-0.00847570	-7.42722977	-1.29902644
H	-1.65472657	-7.58980147	-2.70490121
H	1.53572381	-6.99210363	0.16620160
H	0.36595179	-8.43229492	-1.50511322